PAPER

A supramolecular bottle-brush approach to disassemble amyloid fibrils

Patrick A. Rühs, Jozef Adamcik, Sreenath Bolisetty, Antoni Sánchez-Ferrer and Raffaele Mezzenga*

We present a new strategy to disassemble amyloid fibrils consisting of a supramolecular attachment along the fibrils' contour length of end-terminated counter charged hydrophilic polymers. We chose as a model system to work with positively charged β-lactoglobulin fibrils (pH 2), to which sulfonic acid terminated poly(ethylene glycol) (PEG) chains are ionically attached. The attachment of PEG to the β-lactoglobulin fibrils was confirmed by electrophoretic mobility measurements and small-angle neutron scattering (SANS). This complexation results in a supramolecular bottle-brush system, in which the PEG chains, attached at high grafting densities, stretch out due to excluded volume interactions. The increase in free energy resulting from this entropy loss causes the amyloid fibrils to disassemble, which in turn allows the chains to relax. The decrease in the average contour length of the fibrils was analyzed with atomic force microscopy (AFM) by varying the molecular weight and concentration of the supramolecularly attached polymer. The resulting average contour length distributions were fitted by a Boltzmann distribution law, which yielded an average energy per unit length of the amyloid fibrils. The dependence of this energy on the molecular weight (M_w) and the grafting density of the attached polymers was calculated and compared with available polymer bottle-brush theories. Both the increase in M_w and grafting density the polymer led to a decrease in average contour length. In particular, the characteristic exponent of the M_w-dependence of the energy was found to be identical (0.51) to predictions by Semenov (0.50 in *Polym. Sci. Ser. A*, 2007) and close to predictions by Wang and Safran (0.375 in *J. Chem. Phys.*, 1988). The present findings demonstrate the dynamic association among amyloid fibril building blocks and offer a new appealing supramolecular route to tune their thermodynamic characteristics and their structural properties.

Introduction

Protein aggregates in the form of amyloid fibrils have received substantial interest in various fields of research including medicine,[1] nanotechnology,[2] food and soft materials sciences.[3] The most known example of amyloid fibrils are those directly related to several neurodegenerative diseases including Alzheimer's[4] and Parkinson's[5] diseases. Understanding the physical properties and the formation process of these fibrils is steadily attracting increasing interest to antagonize these diseases, but also to design functional materials.[2,6,7] Indeed, protein fibrils are not always harmful. They can be found in cells as actin and tubulin elements where they support cell growth and structure.[8] Protein fibrils can also be formed by manipulating their physical and chemical environment[2,9–16] or by genetic modification, leading to fibrils with additional binding sites and unconventional properties.[17] Amyloid fibrils, stabilized by hydrogen bonds between parallel β-sheets,[18,19] have great potential as functional nanobiomaterials by possessing very versatile and interesting properties including

high mechanical strength and well defined nanostructures.[2,20] A particular interesting method to prepare rigid, semiflexible fibrils, typically 2–10 nm in diameter, is through the unfolding and aggregation processes of globular proteins.[20,21]

Several different proteins including insulin[11,15] and lysozyme[16] can form fibrils. One food grade protein, which is able to form fibrils upon denaturation is β-lactoglobulin.[22]

β-Lactoglobulin is a globular protein (162 amino acids, 18 400 g mol⁻¹) constituted by an internal core with mostly hydrophobic amino acid sequences while hydrophilic residues are found on the surface of the protein. At pH 2 β-lactoglobulin has a charge of +20e and is found predominantly in the monomeric form.[23–25] This protein is of particular interest for the food industry for being one of the primary components of the whey fraction of bovine milk. β-Lactoglobulin is considered a very important and functional ingredient in food processing due to its emulsifying, structuring, and foaming activity.[26–28]

Upon heating of β-lactoglobulin solutions at different pH, different structural morphologies appear ranging from fibrils to spherical micelles or worm like aggregates.[29] If β-lactoglobulin is heated at 90 °C and pH 2 for 5 h at low ionic strength, long and semi-flexible, thin, fibrillar aggregates with 2–10 nm thickness are formed.[29,30] Periodic variations in thickness along their contour

ETH Zurich, Food & Soft Materials Science, Institute of Food, Nutrition & Health, Schmelzbergstrasse 9, LFO, E23, 8092 Zürich, Switzerland. E-mail: raffaele.mezzenga@agrl.ethz.ch

length indicate that these fibrils are actually multi-stranded fibrils with ribbon-like cross-sections.[31] Stirring while heating, typically increases and optimizes fibril production.[32] Indeed, as proposed by Bolder[32] and later confirmed by Akkermans,[33] not all β-lactoglobulin monomers are converted into the fibrils. The conversion rate of monomers into fibril building blocks is regulated by the processing conditions, with a maximum conversion rate typically reported at *ca.* 75%.[30]

Attaching polymers to the backbone of fibrils has a direct impact on their physical and chemical properties.[34–36] In a previous work, for example, we have shown that ionic complexation between sodium dodecyl sulfate and β-lactoglobulin can fine-tune their solubility and pH-responsiveness.[29]

In this study, a supramolecular bottle-brush approach is proposed to disassemble β-lactoglobulin fibrils by ionically attaching sulfonic acid (negatively charged) terminated poly(ethylene glycol) (PEG) chains onto the positively charged β-lactoglobulin fibrils. Amyloid fibrils have been shown to disassemble *via* different approaches, such as high pressure homogenization,[30] ultrasonication,[37] enzymatic degradation,[38] chemical dissection,[39,40] cold atmospheric plasmas[41] and laser beam irradiation.[42,43] To our knowledge this is the first time a supramolecular bottle-brush approach is proposed to this end.

The formation of a supramolecular bottle-brush was confirmed by electrophoretic mobility of β-lactoglobulin fibrils/PEG complexes and their small-angle neutron scattering analysis. In order to analyse the disassembly of β-lactoglobulin fibrils, the average contour length of β-lactoglobulin was measured by statistical analysis of single-molecule AFM images and compared with the same system after the complexation with PEG. To investigate the systematic decrease in the average contour length, three different molecular weights and six different concentrations of PEG were used. The experimental results were compared to existing bottle-brush theories.

Experimental details

Materials

A 10 w/w% solution of BioPURE β-lactoglobulin (Davisco, Foods International. Inc, Le Sueur, MN) was prepared with MilliQ water. The solution was adjusted to pH 4.6 with 1 M HCl (Merck, CH). After centrifugation (15 000 rpm, 15 min, 20 °C), the supernatant was recovered, adjusted to pH 2, and filtered through a 0.22 μm membrane to remove insoluble protein. This filtered solution was dialyzed with a 6000–8000 MWCO membrane (Spectrum Laboratories, Inc., CA) at first against pH 2 water and then against MilliQ water. The membranes were previously treated with a 1 mM EDTA solution to remove excess ions. The membranes were placed in water baths containing at least 40 times the dialyzed volume. The water baths were changed 8 times over the period of 5 days with at least 4 h between bath changes. After dialysis the pH was adjusted back to pH 2. The β-lactoglobulin solution, containing only native protein from dialysis, was heated at 90 °C while stirring for 5 h using an oil bath according to the procedure described in the following protocol.[29] After heating, the fibrils were stored at 4 °C. Due to the high amount of β-lactoglobulin not converted into fibrils (~25%),[30] the solution was dialyzed a second time to remove excess unreacted protein. The solution was dialyzed against pH 2 water in a 100 000 MWCO membrane (Spectrum Laboratories, Inc., CA). The bath was changed every 1–2 days for 7 days.

Complexation and sample preparation of β-lactoglobulin with PEG

Three different molecular weights (M_w: 750, 2200 and 5000) and 6 different concentrations (from 0.055 mM to 24 mM) of sulfonic acid terminated PEG were used (Table 1). Experiments were carried out in three sets and found to be reproducible. The sulfonated poly(ethylene glycol) monomethyl ether PEG 2200 was commercially available (Polymer Source Inc.). The other two sulfonated polymers (PEG 750 and PEG 5000) were synthesized from the corresponding hydroxyl terminated poly(ethylene glycol) monomethyl ether (Aldrich) when reacting with 1,3-propane sultone and sodium hydride in anhydrous THF.[44–46] The free sulfonic acid polymer derivative was obtained by bubbling HCl to a solution of the polymer sodium salt in THF and filtering of the salts. The concentration of β-lactoglobulin was maintained constant in all samples (0.1 w/w%). Samples were incubated over night at room temperature. The AFM samples were prepared by depositing 20 μl of the sample on a freshly cleaved Mica (Ted Pella, Inc., CA) for 2 min, rinsed with 1 ml of MilliQ water and dried with nitrogen gas.[31]

Statistical analysis with AFM

The NanoScope V MultiMode scanning probe microscope (Veeco Instruments Inc.) was used in tapping mode to avoid contact with the sample surface. Images (1–3) were taken at a resolution of 1024 × 1024 pixels per sample with tips from Veeco (model: Tap150A) at a scan rate of 1 Hz. The coordinates of fibrils on the substrate were acquired using Ellipse software.[31,47] For each image 100 to 500 fibrils were counted and analyzed. The coordinate data acquired by Ellipse were further processed with Mathematica (Wolfram Research Inc.) to yield the contour length of the fibrils.

Transmission electron microscopy (TEM)

The complexes formed by β-lactoglobulin and PEG were imaged using transmission electron microscopy (TEM). Undiluted samples were imaged on glow discharged carbon coated copper grids. Sample grid preparation was as follows: 4 μL sample dispersion for 1 min, 2 μL 2% uranyl acetate for 1 s, and 2 μL 2% uranyl acetate for 15 s. Following each step, the excess moisture was drained along the periphery using filter paper. Dried grids were examined under vacuum by bright field TEM (FEI, model

Table 1 Summary of samples prepared for AFM measurements (final concentrations)

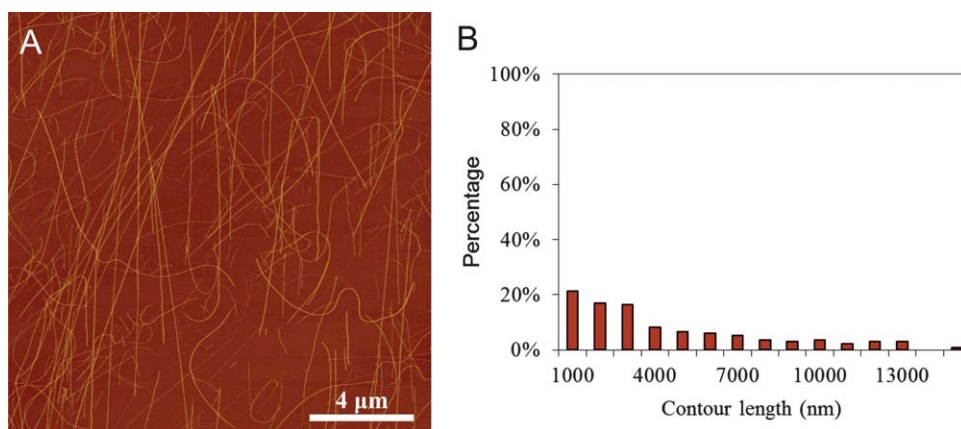| Sample	β-lg (w/w%)	PEG (mM)
PEG 750, PEG 2200, PEG 5000	0.1	0.055
	0.1	0.54
	0.1	1.60
	0.1	8.00
	0.1	16.00
	0.1	24.00

Fig. 1   A: AFM image of β-lactoglobulin fibrils at 0.1 w/w%. B: Average contour length distribution of β-lactoglobulin fibrils.

CM12, NL), operated at a voltage of 100 kV. The brightness and contrast of the pictures were slightly adjusted.

Electrophoretic mobility

The complexation of PEG to the β-lactoglobulin amyloid fibrils was investigated by electrophoretic mobility measurements. The measurements were carried out on a Malvern Nano sizer ZS. The samples were filled into disposable ζ-potential cuvettes (DTS-1030) without air bubble formation. The measurements were performed in back scattering mode at an angle of detection 173°. Electrophoresis measurements directly measure the velocity of the particles moving in electric field using the laser doppler velocimetry (LDV).

Small-angle neutron scattering (SANS)

SANS measurements were performed at the SANS II facility of the SINQ Swiss Neutron source at the Paul Scherer Institute (PSI), Switzerland. Quartz cells (1 mm) from Hellma were used. Combinations of different wavelengths (4.55 and 6.37 Å^{-1}), sample-to-detector distances (1.2–3 m) and collimation lengths (2–6 m) resulted in an effective q range of 0.04–3 nm^{-1}. The raw spectra were corrected for background from the solvent (D$_2$O), empty cell and electronic noise by conventional procedures. The two-dimensional isotropic scattering spectra were corrected for detector efficiency according to standard SANS II data reduction procedure. The resulting neutron scattering intensity *versus* scattering vector was obtained by performing azimuthal averages. For these experiments the samples were prepared in deuterated water (D$_2$O) in order to provide sufficient contrast to neutrons. Concentrations ranging from 0.1 to 0.3 w/w% were used in order to probe directly the form factor of the aggregates under investigation.

Results

The β-lactoglobulin fibrils have an average contour length of 4390 nm and an average persistence length of 2450 nm. The histogram of these fibrils displays a typical polydisperse distribution, as shown in Fig. 1.

After the addition of PEG, the fibril average contour length decreases (Fig. 2). The TEM images show that the fibrils are shorter and have an increased tendency to aggregate.

This effect was confirmed and analysed in more details by single-molecule AFM analysis. The decreasing effect on the average contour length was measured at three different molecular weights of PEG and six different concentrations. Representative images of this analysis are shown in Fig. 3: it is clear that at the same molar concentration of PEG the average contour length of the fibrils decreases when increasing the molecular weight of the PEG (Fig. 3A, 3B and 3C). Similarly, for any given PEG molecular weight, the contour length decreases when the PEG molar concentration is increased (Fig. 3: left *versus* right columns).

The average contour length was measured as described in the Experimental part. In Fig. 4 the resulting average contour length, normalized to that of uncomplexed β-lactoglobulin fibrils, is presented at different concentration of PEG and for the different molecular weights considered.

Over all concentrations (from 0.055 mM to 24 mM) the steady decrease in the average contour length with PEG concentration and molecular weight is evident. From Fig. 4 it is clear that at the highest concentration of PEG (24 mM), complexation with PEG 2200 and PEG 5000 has led to a decrease of the average contour length by more than a factor two.

The length distributions for various PEG complexes (at constant molar concentration) and various PEG concentrations (and fixed molecular weight) are shown in Fig. 5a and 5b, respectively. A clear shift from longer to shorter fibrils is found upon increase of either molecular weight (Fig. 5a) or concentration (Fig. 5b), *e.g.* the population of shorter fibrils increases. Additionally, the populations of fibrils with the largest contour
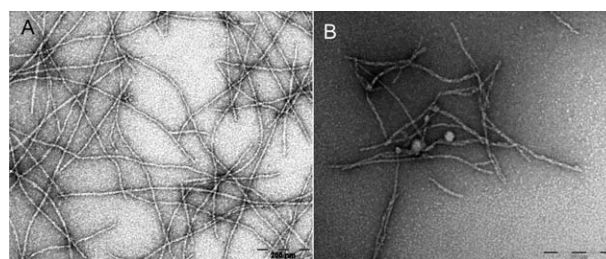

Fig. 2   TEM images of β-lactoglobulin fibrils without (**A**) and with (**B**) PEG 2200. Scale bars are 200 nm.
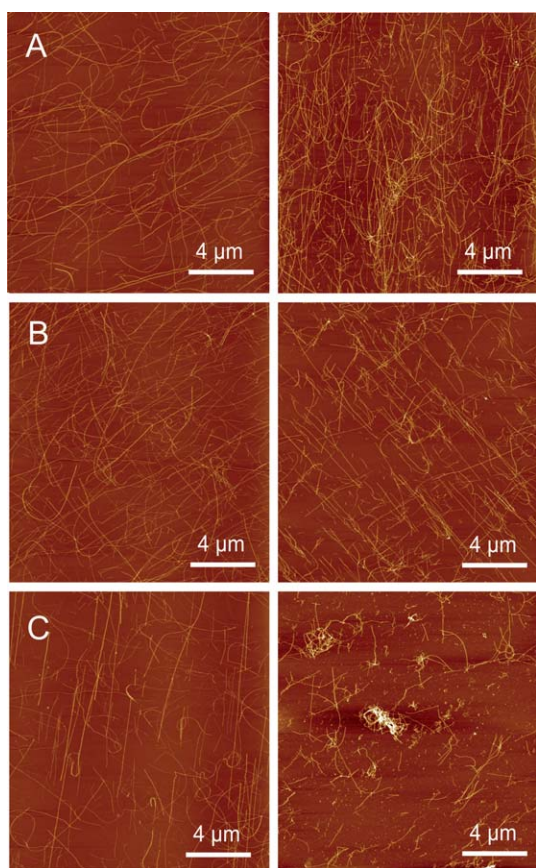
Fig. 3 AFM images of β-lactoglobulin with PEG, A: M_w 750, B: M_w 2200, C: M_w 5000. From left to right the concentration of PEG is 0.055 mM and 24 mM, respectively.
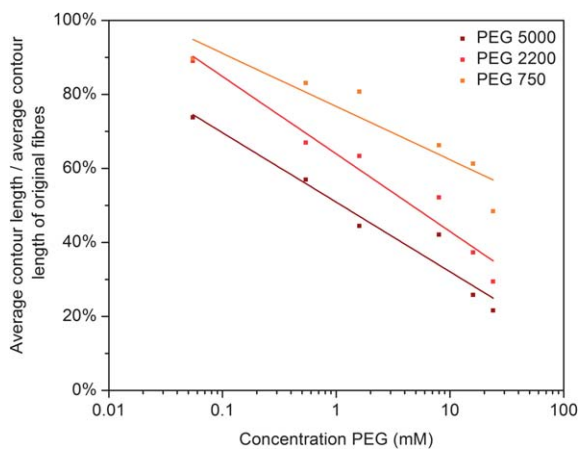

Fig. 4 Average contour length (normalized to that of uncomplexed fibrils) *versus* molar concentration of PEG for β-lactoglobulin fibrils ionically complexed with sulfonic-terminated PEG of molecular weights 750, 2200 and 5000 g/mol.

lengths extinct rapidly with either PEG concentration or molecular weight increase.

In order to provide insight on the nature of interactions between the PEG and the protein fibrils, the complexation of PEG (M_w: 2200) to the β-lactoglobulin fibrils was investigated by
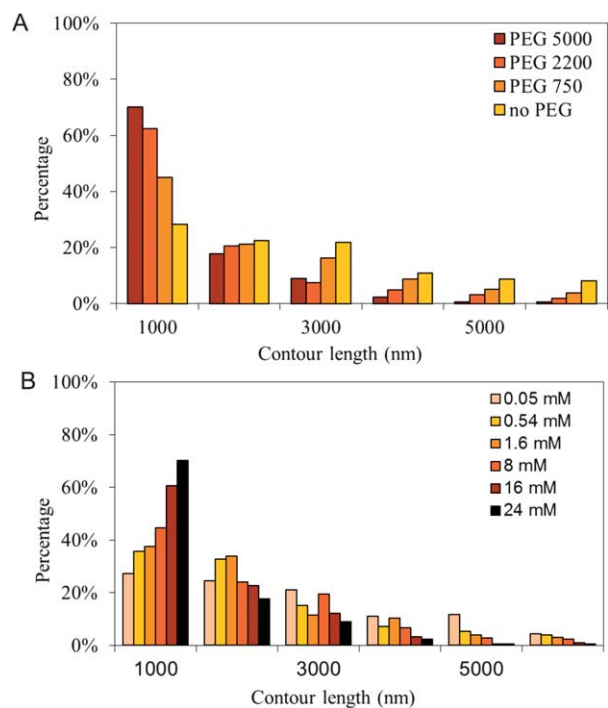

Fig. 5 Contour length distribution of fibrils at fixed PEG concentration (24 mM) with attached PEG of various molecular weights (**A**). Contour length distribution of fibrils at fixed PEG molecular weight (5000 Dalton) and varying molar concentrations (**B**).

electrophoretic mobility. Control experiments with non-charged PEG showed no effect on the electrophoretic mobility. Fig. 6 presents the change in electrophoretic mobility depending on different molar concentrations of PEG. Below 0.1×10^{-3} mol l^{-1} PEG concentration, the electrophoretic mobility is constant,
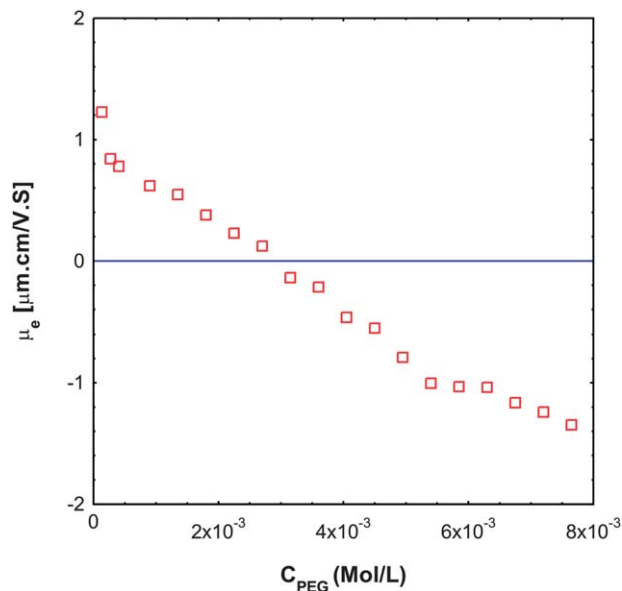

Fig. 6 Electrophoretic mobility of β-lactoglobulin fibrils (0.001 w/w%) upon progressive complexation with PEG (M_w: 2200) at increasing molar concentration ratios.

unaffected by the concentration of PEG. Although complexation occurs, higher concentration of PEG is required to diminish the total net charge of the β-lactoglobulin fibrils. As the concentration of PEG increases, the electrophoretic mobility decreases gradually. At a concentration of 3×10^{-3} mol l^{-1}, the measured electrophoretic mobility is zero. This indicates that the surface of the β-lactoglobulin fibrils is completely neutralized. Remarkably, at this concentration, the β-lactoglobulin fibril:PEG complexes are still soluble in water, which already provides a very strong evidence of bottle-brush complexes. Further increase in concentration of PEG results in an inversion of charge and a total net negative charge on the surface of complexes is measured, indicating the excess PEG, in a mechanism similar to what already discussed in our earlier work using sodium dodecyl sulphate surfactant.[29] In conclusion, these results clearly indicate that negatively end-terminated PEG chains do attach to the surface of the positively charged β-lactoglobulin fibrils.

Small angle neutron scattering was employed to further elucidate the detailed structure of the β-lactoglobulin fibrils-PEG complexes. Fig. 7a and 7b clearly demonstrate that the complexation of PEG to β-lactoglobulin amyloid fibrils causes a dramatic change of the SANS spectra. Fig. 7a shows that in the q range of 0.1–0.5 nm^{-1}, the scattering intensity follows the asymptotic slope of −1, which reveals the β-lactoglobulin rod-like structure at these length scales. At higher q region the scattering curve follows decays faster, probing the cross-section of the fibrils. The flexibility of β-lactoglobulin fibrils, radius of the cross-section and detailed information of the form factor of these fibrils has been already discussed extensively in our previous work.[29]

The SANS spectra (I vs. q) of β-lactoglobulin amyloid fibrils complexed with PEG 2200 is shown in Fig. 7b. Remarkably, in the q region 0.1 to 1 nm^{-1} the q^{-1} and higher slope decay regimes have been replaced by a plateau, as a result of the complexation. To obtain more quantitative information on the structure of these complexed β-lactoglobulin fibrils, we modelled the SANS data using polydisperse cross-section core–shell cylinders. The

fitting routine used is that provided by NIST[48] and is based on the model of polydisperse core–shell cylinders derived by Guinier.[49] Here we only quote the relevant equations used in the model to fit the experimental data.

The total scattered intensity is:

$$I(q) = \frac{scale}{V_p} \sum_{R_p} n(R_p, \sigma_p) P(q, R_p, R_l, H_p, H_l, \rho_p, \rho_l, \rho_{sol}) \quad (1)$$

where the normalized distribution of cylinders with core radius R_p, mean core radius is R_0 and polydispersity σ_p is expressed by:

$$n(R_p) = \frac{\exp\left[-\frac{1}{2}\left(\frac{\ln(R_p/R_0)}{\sigma_p}\right)^2\right]}{\sqrt{(2\pi)}\sigma_p R_p} \quad (2)$$

and the form factor of each individual core–shell cylinders is:

$$P(q) = \int_0^{\frac{\pi}{2}} \sin\theta\,\partial\theta \cdot \left[V_1(\rho_l - \rho_{solv}) \frac{\sin\left(\frac{qH_l\cos\theta}{2}\right)}{\frac{qH_l\cos\theta}{2}} \frac{2J_1(qR_l\sin\theta)}{qR_l\sin\theta} \right.$$
$$\left. + V_p(\rho_p - \rho_l) \frac{\sin\left(\frac{qH_p\cos\theta}{2}\right)}{\frac{qH_p\cos\theta}{2}} \frac{2J_1(qR_p\sin\theta)}{qR_p\sin\theta} \right]^2 \quad (3)$$

in which $J_1(x)$ is the first order Bessel function, the angle θ is defined as the angle between the cylinder axis and the scattering vector q. The integral over theta averages the form factor over all possible orientations of the cylinder with respect to q. The additional terms in eqn (1)–(3), V, H, ρ stand for the volume, the length and the density, and the indexes p, l and $solv$ identify the core, the shell and the solvent, respectively.
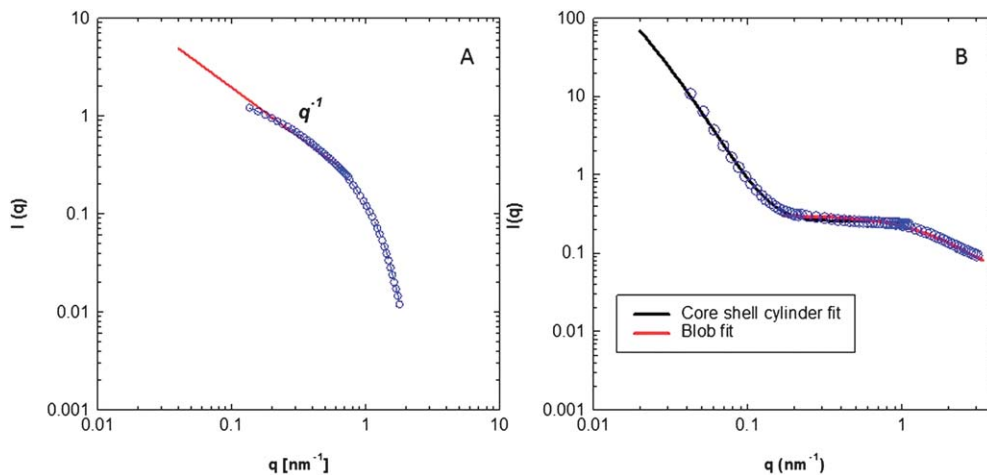

Fig. 7 Small-angle neutron scattering intensities $I(q)$ vs. the scattering vector (q) for the β-lactoglobulin fibrils. (A) Uncomplexed β-lactoglobulin fibrils: the solid line (slope of −1) indicates a rod-like structure. (B) Complexed β-lactoglobulin: the SANS intensity curve of the complexes of the 0.1 w/w% β-lactoglobulin amyloid fibrils with 4.5×10^{-2} mol l^{-1} complexed PEG. The solid line is the fit of the experimental data using a combination of polydisperse core shell cylindrical model and blob fluctuations at larger scattering vectors.

The form factor $P(Q)$ is normalized by multiplying by a factor referred as $scale/V_p$. When $scale$ represents the volume fraction of the core particles then the multiplication factor is the number density of particles and an absolute intensity is obtained.

Additionally, to the above analysis, bottle-brush polymers scattering intensities are dominated by extra contributions at high scattering vectors due to internal density fluctuations—also called blob scattering[50,51]—and thus, the scattering contribution due to internal density fluctuations is modelled in what follows using the Dozier approach:[52]

$$I(q) = P(q) + a_b \frac{\sin\left[\mu \tan^{-1}\left(q_b^*\right)\right]}{\mu q_b^* \left[1 + q_b^{*2}\right]^{\mu/2}} \quad (4)$$

with

$$q_b^* = \frac{q\xi}{\left[\text{erf}(qR_c/\sqrt{6})\right]^3} \quad \text{and} \quad \mu = \frac{1}{v_b} - 1 \quad (5)$$

where v_b is the Flory exponent, ξ is the correlation length of blob, erf denotes the error function. The amplitude a_b is the scattering due to thermal fluctuations relative to the amplitude of the contribution resulting from the overall shape ($P(q)$).

The fit of polydisperse core–shell cylinders is shown as a solid curve in the low q region (0.02–1 nm^{-1}) of Fig. 7b. The parameters used for the fits are: shell thickness of 3 nm, average contour length of 800 nm, core radius of 6 nm and standard deviation of 0.9. The internal density fluctuations (blob scattering) fits are shown as dashed lines in Fig. 7b in the remaining high q-region. The parameters used for the blob scattering fits are: radius of cross section of 6 nm, blob scattering amplitude a_b of 0.3, blob correlation length of 1 nm.

The SANS data of PEG-complexed amyloid fibrils fit very well with the model of polydisperse core–shell cylinders in the low q region (higher length scales) having scattering contributions from blobs fluctuations at higher q (lower length scales). This confirms the topological model of a polymer bottle-brush structure with a thick core, which is also in line with the structural model inferred by the electrophoretic mobility measurements.

Discussion

The contour length of the uncomplexed fibrils and their polydispersity is comparable to those measured by other authors.[14,31] After ionic complexation with PEG polymers, the average fibril contour length diminishes. In what follows, and based on the experimental evidence provided above, we discuss and interpret this disassembly process by means of bottle-brush theories.

The β-lactoglobulin fibrils are positively charged, with a total charge per monomer of +20e at pH 2.[24] Thus, the negatively end-charged PEG molecules (at pH 2) bind to the positive backbone of the fibril as sketched in Fig. 8.

The structure of the brush polymer is a result of interactions between the β-lactoglobulin fibrils and the PEG. At low grafting densities, the PEG molecules will attach to the β-lactoglobulin fibrils forming mushroom-like structures (Fig. 8a); however at higher grafting densities a bottle-brush system will be formed (Fig. 8b). According to Alexander–de Gennes,[53] a flat macromolecular brush, with a constant correlation length (or blob size)

is formed when the distance between grafting points D is smaller than the radius of gyration of the unattached chain. In the present case, the distance between the different grafting points of the fibril is small enough to enable interactions between the PEG molecules. Due to the fact that PEG has a more extended configuration than the globular β-lactoglobulin protein, it is then reasonable to expect closely packed grafted PEG chains emanating out of the β-lactoglobulin fibrils backbone for all the PEG considered. This densely crowded brush will cause the PEG chains to stretch out due to excluded volume interactions in a good solvent, which in the present case is simply water.[54] This highly stretched configuration of PEG chains, compared to the unattached PEG, results in a loss of configurational entropy of the chains, and thus, in an increase of the total free energy $\Im$ per unit length associated to the supramolecular bottle-brush fibrils.[55] The only way bottle-brush β-lactoglobulin amyloid fibrils have to release the stretching penalty, and thus to reduce the free energy, is to break down in smaller pieces, so that the space associated with the fibrils extremities will become increasingly available to relax PEG stretching frustration. This break down process—which by any experimental evidence occurs in the present system—is the one-dimensional analogue of the two dimensional process leading to the stabilization of hairy hockey pucks *versus* infinite monolayers, already discussed by Fredrickson *et al.*[56] The break-down process, however, does not proceed indefinitely because reduction of the contour length is also associated with the loss of the (negative) binding energy U associated with the hydrogen bonded β-sheets holding together the amyloid fibrils. A formal treatment of this problem would then require the exact minimization of the total free energy F = $\Im$-U.

In what follows we adopt a different procedure, which has the advantage to avoid the complications associated with the exact minimization of the total free energy.

A theoretical description of the free energy per unit length for bottle-brush polymers in a good solvent, was derived by Wang and Safran.[57] According to their work, the free energy per unit length is:

$$\beta\Im \sim a^{-1}\sigma^{13/8}M^{3/8} \quad (6)$$

where β is equal to $\frac{1}{k_B T}$, $k_B T$ being the thermal energy, M the degree of polymerization of the attaching chain, σ is grafting density of the side-chain polymers, and a is the normalized diameter of one monomer.[55] A similar equation was derived by Semenov[58] who proposed a slightly different free energy per unit length:

$$\Im \sim a^{-1}\sigma^{3/2}M^{1/2}\sqrt{v} \quad (7)$$

where v is the second virial coefficient of the monomers composing the side chains. The other parameters are the same as defined in eqn (6).

Both authors found that the free energy is dependent on the grafting density and the degree of polymerization, *via* exponents, which differ only slightly in the two theories. Differently from the Alexander–de Gennes brush, in which the size of polymeric blobs
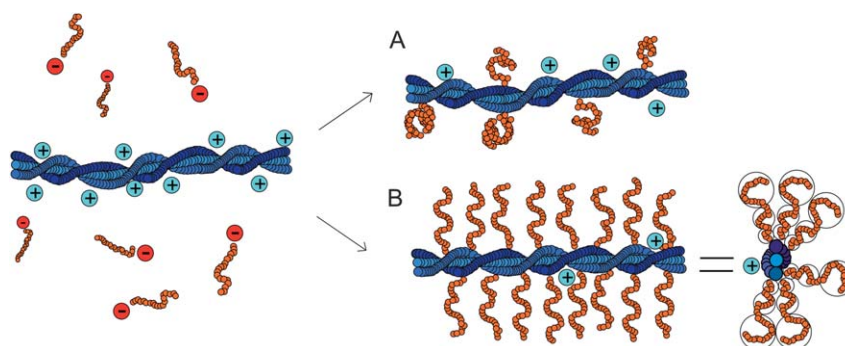
Fig. 8 Schematic diagram illustrating the ionic complexation between the positive backbone of the β-lactoglobulin fibrils and the negatively end-charged PEG chains. Mushroom regime is expected at low grafting densities (**A**), whereas bottle-brush regime is to be found at high grafting densities (**B**).

remains constant along the brush thickness, in the case of bottle-brush, the radius of the blobs of the attached polymer chains increases when increasing the distance from the backbone (see Fig. 8).

Because eqn (6) and eqn (7) give the free energy per unit length of a bottle-brush system, the energy F of each surviving fibril having contour length l is simply $l \cdot (\Im\text{-}U)$, where again U is the total h-bonding binding energy per unit length of the amyloid fibril.

One can realistically assume a Boltzmann distribution of states for the fibrils,[59] so that the probability to find a fibril of an energy $l \cdot (\Im\text{-}U)$, which is also the probability to find a fibril of length l, is:

$$P(l) \approx e^{-\frac{(\Im - U) \cdot l}{k_B T}} \tag{8}$$

The value of $\Im\text{-}U$ for the different molecular weights and concentrations (grafting density) of PEG can be extracted by fitting eqn (8) against the corresponding contour length distribution, such as those shown in Fig. 5. An example of this fit is shown in Fig. 9a and 9b, in which, the expected exponential behaviour *versus* the contour length expressed by eqn (8) is nicely confirmed against experimental data.

By developing $\Im\text{-}U$ in eqn (8), in which $\Im$ is that predicted by either eqn (6) (Wang and Safran) or 7 (Semenov), one obtains:

$$P \approx e^{(a^{-1}\sigma^x M^y - U)^x l} \tag{9}$$

where U and a are unknown parameters whose physical meaning has been discussed above, but which do not embody the molecular weight and grafting density dependence of the supramolecular bottle-brush free energy. The exponents x and y, however, capture directly the dependence of the free energy of the bottle-brush (and thus the observable contour length distribution) on the grafting density and molecular weight of the side chains. The exponent $\tau = a^{-1} \cdot M^y \sigma^x - U$ in eqn (9) can be determined by fitting the specific contour length distribution corresponding to any of the eighteen experimental cases considered (six concentrations times three molecular weight), as shown in Fig. 9. In any case, either M or σ is changed. There are 18 experimental values τ_{EXP}, which are then interpreted by a four-parameter varying $\tau(a^{-1}, U, x, y)$.

The four parameters a^{-1}, U, x, y can then be obtained by finding the least square of $\Sigma_{M,\sigma} [\tau(a^{-1}, U, x, y) - \tau_{EXP}]^2$ and comparing directly x and y with the values predicted by Wang & Safran and Semenov. To perform this analysis we have used the FindFit function of Mathematica (Wolfram Inc.).

The exponent x, expressing the concentration dependence, obtained by the analysis discussed above, was 0.39. Although this value qualitatively captures the observed increase of energy with grafting density, it is rather small compared to the values predicted by Wang & Safran (1.625) and Semenov (1.5).

This is however expected, since in order to apply bottle-brush theories developed for covalent bottle-brush systems, we have
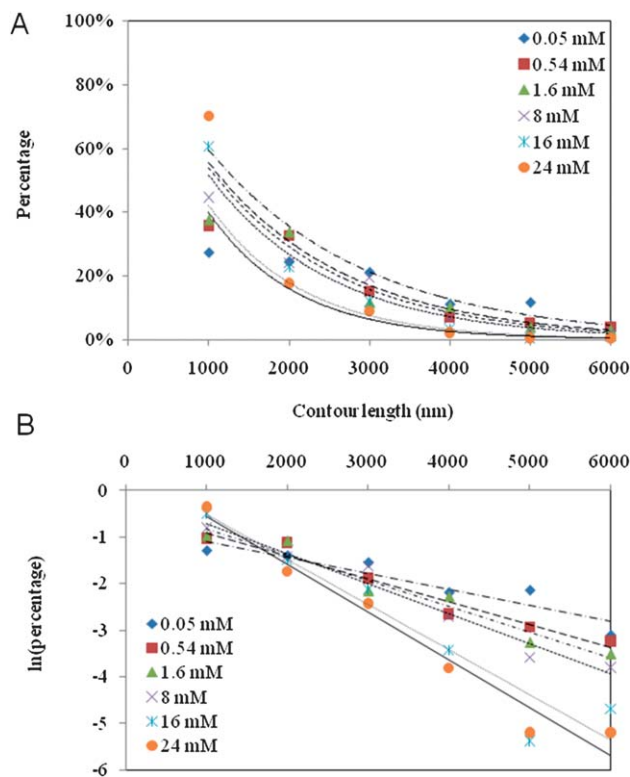

Fig. 9 Exponential fit (**A**) and semi-log fit (**B**) of the contour length distribution of β-lactoglobulin fibrils with different concentrations of PEG 5000 using the Boltzmann distribution function (eqn (8)).

been obliged to assume that the molar concentration of PEG in bulk is directly proportional to the grafting density σ, which is a very strong assumption. In reality competition of steric over-crowding of PEG chains and electrostatic interaction between the PEG and the fibrils make the dependence of σ on the bulk molar concentration of PEG much weaker than linear, which is directly reflected by the lower experimentally determined exponent x.

More interesting and directly comparable to the theory is the exponent y reflecting the molecular weight dependence, since this is not sensitive to differences between a supramolecular and a covalent bottle-brush. Our least square analysis determined an exponent y of 0.51 which is identical to what predicted by Semenov (0.5), and close to predictions of Wang & Safran (0.375). This is a further, strong evidence that the main mechanism responsible for amyloid fibrils breakage is the energy penalty associated with the supramolecular bottle-brush.

Finally, we observe that the binding of side chains to the backbone of amyloid fibrils is also expected to decrease flexibility of the β-lactoglobulin fibrils in agreement with theoretical predictions for highly dense bottle-brush systems.[55,60] Nonetheless, because fibrils rapidly break upon PEG attachment, their contour length promptly falls below the characteristic persistence length, which makes the statistic evaluation of the persistence length variation very poor and the study unfeasible in the present system.

Conclusions

We have investigated the effect of the ionic complexation of β-lactoglobulin fibrils with sulfonic acid terminated PEG at different molecular weights and different concentrations. By using single molecule atomic force microscopy and statistical analysis, the average contour length was analysed before and after the complexation. The complexation was demonstrated by electrophoretic mobility measurements and small angle neutron scattering. There is clear evidence that the complexation of PEG leads to a decrease in average contour length. A supramolecular bottle-brush is formed at high grafting densities through this complexation. This causes the side-chain polymers to stretch due to excluded volume interaction, reducing their configurational entropy and increasing the supramolecular bottle-brush free energy. As a result, the fibrils break to relax at the chain ends some of the stretching of side-chain polymers. The resulting fibril length distributions were fitted with the Boltzmann distribution function and the results were then compared with existing bottle-brush theories from Wang & Safran and Semenov. The side-chain molecular weight dependence of the free energy of the bottle-brush fibrils is very close or identical (depending on the theory considered) to the effect proposed by these authors, whereas the effect of concentration is weaker than theoretical predictions, as a consequence of the supramolecular binding of the side-chain polymers.

Taken together, these results indicate that ionic binding of charge-terminated hydrophilic polymers with counter charged amyloid fibrils can be used as a new efficient supramolecular strategy to the disassemble amyloid fibrils and that insightful information regarding the total binding energy holding together amyloid fibrils can be gained by applying existing polymer bottle-brush theories.

References

1 C. M. Dobson, *Nature*, 2003, **426**, 884–890.
2 I. Cherny and E. Gazit, *Angew. Chem., Int. Ed.*, 2008, **47**, 4062–4069.
3 D. Oboroceanu, L. Z. Wang, A. Brodkorb, E. Magner and M. A. E. Auty, *J. Agric. Food Chem.*, 2010, **58**, 3667–3673.
4 P. K. Chiang, M. A. Lam and Y. Luo, *Curr Mol Med*, 2008, **8**, 580–584.
5 G. B. Irvine, O. M. El-Agnaf, G. M. Shankar and D. M. Walsh, *Mol. Med.*, 2008, **14**, 451–464.
6 D. J. Selkoe, *Nature*, 2003, **426**, 900–904.
7 J. D. Sipe and A. S. Cohen, *J. Struct. Biol.*, 2000, **130**, 88–98.
8 P. L. Graumann, *Annu. Rev. Microbiol.*, 2007, **61**, 589–618.
9 R. Jansen, S. Grudzielanek, W. Dzwolak and R. Winter, *J. Mol. Biol.*, 2004, **338**, 203–206.
10 H. X. Zhao, E. K. J. Tuominen and P. K. J. Kinnunen, *Biochemistry*, 2004, **43**, 10302–10307.
11 J. L. Whittingham, D. J. Scott, K. Chance, A. Wilson, J. Finch, J. Brange and G. G. Dodson, *J. Mol. Biol.*, 2002, **318**, 479–490.
12 P. Rasmussen, A. Barbiroli, F. Bonomi, F. Faoro, P. Ferranti, M. Iriti, G. Picariello and S. Iametti, *Biopolymers*, 2007, **86**, 57–72.
13 A. Kroes-Nijboer, P. Venema, J. Bouman and E. van der Linden, *Food Biophys.*, 2009, **4**, 59–63.
14 L. M. C. Sagis, C. Veerman and E. van der Linden, *Langmuir*, 2004, **20**, 924–927.
15 E. J. Nettleton, P. Tito, M. Sunde, M. Bouchard, C. M. Dobson and C. V. Robinson, *Biophys. J.*, 2000, **79**, 1053–1065.
16 M. R. H. Krebs, D. K. Wilkins, E. W. Chung, M. C. Pitkeathly, A. K. Chamberlain, J. Zurdo, C. V. Robinson and C. M. Dobson, *J. Mol. Biol.*, 2000, **300**, 541–549.
17 T. Scheibel, R. Parthasarathy, G. Sawicki, X. M. Lin, H. Jaeger and S. L. Lindquist, *Proc. Natl. Acad. Sci. U. S. A.*, 2003, **100**, 4527–4532.
18 M. F. Perutz, J. T. Finch, J. Berriman and A. Lesk, *Proc. Natl. Acad. Sci. U. S. A.*, 2002, **99**, 5591–5595.
19 A. T. Petkova, Y. Ishii, J. J. Balbach, O. N. Antzutkin, R. D. Leapman, F. Delaglio and R. Tycko, *Proc. Natl. Acad. Sci. U. S. A.*, 2002, **99**, 16742–16747.
20 S. Kumar and J. B. Udgaonkar, *Curr Sci India*, 2010, **98**, 639–656.
21 W. S. Gosal, A. H. Clark, P. D. A. Pudney and S. B. Ross-Murphy, *Langmuir*, 2002, **18**, 7174–7181.
22 L. N. Arnaudov, R. de Vries, H. Ippel and C. P. M. van Mierlo, *Biomacromolecules*, 2003, **4**, 1614–1622.
23 G. Kontopidis, C. Holt and L. Sawyer, *J. Dairy Sci.*, 2004, **87**, 785–796.
24 F. Fogolari, L. Ragona, S. Licciardi, S. Romagnoli, R. Michelutti, R. Ugolini and H. Molinari, *Proteins: Struct., Funct., Bioinf.*, 2000, **39**, 317–330.
25 P. Aymard, D. Durand and T. Nicolai, *Int. J. Biol. Macromol.*, 1996, **19**, 213–221.
26 C. Veerman, L. M. C. Sagis and E. van der Linden, *Macromol. Biosci.*, 2003, **3**, 243–247.
27 S. R. Euston, S. Ur-Rehman and G. Costello, *Food Hydrocolloids*, 2007, **21**, 1081–1091.
28 A. H. Clark, G. M. Kavanagh and S. B. Ross-Murphy, *Food Hydrocolloids*, 2001, **15**, 383–400.
29 J. M. Jung, G. Savin, M. Pouzot, C. Schmitt and R. Mezzenga, *Biomacromolecules*, 2008, **9**, 2477–2486.
30 J. M. Jung and R. Mezzenga, *Langmuir*, 2010, **26**, 504–514.
31 J. Adamcik, J. M. Jung, J. Flakowski, P. De Los Rios, G. Dietler and R. Mezzenga, *Nat. Nanotechnol.*, 2010, **5**, 423–428.
32 S. G. Bolder, L. M. C. Sagis, P. Venema and E. van der Linden, *J. Agric. Food Chem.*, 2007, **55**, 5661–5669.
33 C. Akkermans, P. Venema, A. J. van der Goot, H. Gruppen, E. J. Bakx, R. M. Boom and E. van der Linden, *Biomacromolecules*, 2008, **9**, 1474–1479.

34 F. Huang, R. Rotstein, S. Fraden, K. E. Kasza and N. T. Flynn, *Soft Matter*, 2009, **5**, 2766–2771.

35 K. R. Purdy, S. Varga, A. Galindo, G. Jackson and S. Fraden, *Phys. Rev. Lett.*, 2005, **94**, 057801.

36 I. W. Hamley, M. J. Krysmann, V. Castelletto and L. Noirez, *Adv Mater*, 2008, **20**, 4384–4384.

37 E. Chatani, Y. H. Lee, H. Yagi, Y. Yoshimura, H. Naiki and Y. Goto, *Proc. Natl. Acad. Sci. U. S. A.*, 2009, **106**, 11119–11124.

38 K. Numata and D. L. Kaplan, *Biochemistry*, 2010, **49**, 3254–3260.

39 A. Loksztejn and W. Dzwolak, *Biochemistry*, 2009, **48**, 4846–4851.

40 C. E. MacPhee and C. M. Dobson, *J. Mol. Biol.*, 2000, **297**, 1203–1215.

41 D. L. Bayliss, J. L. Walsh, G. Shama, F. Iza and M. G. Kong, *New J. Phys.*, 2009, **11**, 115024.

42 D. Ozawa, H. Yagi, T. Ban, A. Kameda, T. Kawakami, H. Naiki and Y. Goto, *J. Biol. Chem.*, 2009, **284**, 1009–1017.

43 H. Yagi, D. Ozawa, K. Sakurai, T. Kawakami, H. Kuyama, O. Nishimura, T. Shimanouchi, R. Kuboi, H. Naiki and Y. Goto, *J. Biol. Chem.*, 2010, **285**, 19660–19667.

44 O. Rist and P. H. Carlsen, *Molecules*, 2005, **10**, 1169–1178.

45 P. Renouf, D. Hebrault, J. R. Desmurs, J. M. Mercier, C. Mioskowski and L. Lebeau, *Chem. Phys. Lipids*, 1999, **99**, 21–32.

46 M. Ulewicz, W. Walkowiak, Y. C. Jang, J. S. Kim and R. A. Bartsch, *Anal. Chem.*, 2003, **75**, 2276–2279.

47 J. Marek, E. Demjenova, Z. Tomori, J. Janacek, I. Zolotova, F. Valle, M. Favre and G. Dietler, *Cytometry, Part A*, 2005, **63A**, 87–93.

48 S. R. Kline, *J. Appl. Crystallogr.*, 2006, **39**, 895–900.

49 A. Guinier and G. Fournet, *Small-Angle Scattering of X-Rays*, Wiley, New York, 1955.

50 S. Bolisetty, C. Airaud, Y. Xu, A. H. E. Muller, L. Harnau, S. Rosenfeldt, P. Lindner and M. Ballauff, *Phys. Rev. E: Stat., Nonlinear, Soft Matter Phys.*, 2007, **75**, 040803.

51 S. Rathgeber, T. Pakula, A. Wilk, K. Matyjaszewski and K. L. Beers, *J. Chem. Phys.*, 2005, **122**, 7318.

52 W. D. Dozier, J. S. Huang and L. J. Fetters, *Macromolecules*, 1991, **24**, 2810–2814.

53 P. G. Degennes, *Ann Chim-Rome*, 1987, **77**, 389–410.

54 T. A. Witten and P. A. Pincus, *Macromolecules*, 1986, **19**, 2509–2513.

55 G. H. Fredrickson, *Macromolecules*, 1993, **26**, 2825–2831.

56 D. R. M. Williams and G. H. Fredrickson, *Macromolecules*, 1992, **25**, 3561–3568.

57 Z. G. Wang and S. A. Safran, *J. Chem. Phys.*, 1988, **89**, 5323–5328.

58 A. V. Subbotin and A. N. Semenov, *Polym. Sci.*, 2007, **49**, 1328–1357.

59 J. H. Gibbs, *J. Chem. Educ.*, 1971, **48**, 542.

60 L. Feuz, F. A. M. Leermakers, M. Textor and O. Borisov, *Macromolecules*, 2005, **38**, 8891–8901.